Gamma Ray Bursts and Their Afterglows

Re'em Sari

Theoretical Astrophysics, Caltech 130-33, Pasadena, CA 91125; sari@tapir.caltech.edu

Abstract. Gamma-Ray Bursts are extreme astrophysical events, which emit the bulk of their energy as photons in the $0.1 - 1.0$ MeV range, and whose durations span milliseconds to tens of minutes. They are formed in extreme relativistic outflows with Lorentz factors of hundreds, and reside at cosmological distances. They are followed by X-ray, optical and radio afterglows which can be observed for over a year after the event. Observations of afterglows showed that the emission is from jets, and when corrected for this geometry the energies of GRBs appear to cluster around 5×10^{50} erg – very comparable to that of supernovae. Evidence in the last several years shows that a significant fraction of long GRBs are related to a peculiar type of supernova explosions. These supernovae most likely mark the birth events of stellar mass black holes as the final products of the evolution of very massive stars. Short bursts are still somewhat mysterious, but it is known that some of them are produced by an old population of stars. Neutron star merger is a leading candidate as the progenitor of short GRBs.

Keywords: Gamma-Ray Bursts, Afterglow, Relativistic Jets

THE GENERIC PICTURE

The Burst And Transient Source Experiment (BATSE) on board the Compton Gamma-Ray Observatory observed about one GRB a day over the nineties. BATSE provides a wealth of information on GRB light curves and spectra (Fishman & Meegan 1995) (see also G. Richardson, these proceedings). Some of the key properties are listed below:

- GRBs have durations ranging from milliseconds to $\sim 10^3$ s. The distribution of burst durations is bimodal and separates GRBs into two classes, the short events ($<$2s) and the longer ones ($>$2s) (Kouveliotou et al. 1993). The duration appears to be anticorrelated with spectral hardness: short bursts are predominantly harder than long ones.
- Some GRBs show rapid variability, on time scales of order of a millisecond (Bhat et al. 1992; Schaefer & Walker 1999). It is therefore generally believed that GRBs originate from compact objects, such as neutron stars (NS) or black holes (BH).
- The distribution of the bursts over the sky is uniform to a large degree. Nevertheless, the number of bursts above a flux s falls less steeply than $s^{-3/2}$, which is the expectation from a uniform distribution in Euclidean space.
- High-energy emission is a unique feature of GRBs. The continuum spectra of GRBs are very broad and hard; most of the power is emitted above 50 keV. GRB spectra are well described by an empirical function, the so called Band function (Band et al. 1993). This function consists of a low- and high-energy power law, smoothly joined by an exponential turnover. It has four parameters, the peak energy, the low- and high-energy photon index, and an overall normalization. The high energy photon

CP856, *Relativistic Jets,*
edited by P. A. Hughes and J. N. Bregman

index is close to -2, i.e., roughly equal amount of energy in each decade of photon energy.

On scales of Gpc or more, all objects are distributed roughly isotropically and uniformly. Moreover, a cosmological distribution of sources would reveal a natural deficiency of weaker bursts by relativistic effects that affect the weaker (on average at greater distances) bursts (Paczyński 1986, 1992; Mao & Paczyński 1992). Therefore, it was already in the BATSE days that cosmological distances seemed the most plausible. The energy implied is of order 10^{51} erg.

The observed spectra, energies and timescales of GRBs have lead to a generic model, the so called fireball shock model that is almost independent of the 'inner engine'.

The extreme characteristics of GRBs, lead to a paradox, the so called 'compactness problem'. An energy of 10^{50}erg is released within a variability time $\delta T \sim 0.1$s in the form of photons of about 1 MeV. This translates into the huge number of $N = 10^{56}$ photons. If we now assume that the energy is released in a small volume of linear dimensions $R \leq c\delta T \sim 10^9$cm (which is naively required by the variability timescale), then the optical depth to pair creation would be the number of photons per unit area, multiplied by the Thomson cross section, σ_T, or

$$\tau \sim \sigma_T \frac{N}{4\pi R^2} \sim 3 \times 10^{11} \gg 1.$$

But, if that were true, such a large optical depth implies that all the photons will have created pairs and thermalized. However, the observed spectrum of GRBs is highly non-thermal!

The only known solution to the 'compactness problem' is relativistic motion (Paczyński 1986; Goodman 1986). These effects were considered in detail in Krolik & Pier (1991); Fenimore, Epstein, & Ho (1993); Baring & Harding (1997). A critical review of these as well as some new limits are given by Lithwick & Sari (2001). If the emission site is moving relativistically, with a Lorentz factor γ, toward the observer, then the optical depth is reduced, compared to the stationary estimate, due to two effects. First, the size of the source can be larger by a factor of γ^2. This will still produce variability over a short time scale given by $\delta T = R/\gamma^2 c$ since not all of the source is seen as the radiation for a relativistically moving object is beamed (see Figure 1). Second, the photons in the local frame are softer by a factor of γ, and therefore only a small fraction of them, the ones at the high-energy tail of the GRB spectrum, have enough energy to create pairs. The combination of these two effects reduces the optical depth by a factor of $\sim \gamma^{6.5}$, where the exact power depends on the GRB spectrum (see Lithwick & Sari 2001). Therefore, the optical depth is reduced below unity, and the 'compactness problem' is solved, if the Lorentz factor is larger than about a hundred.

This solution to the compactness problem led to a three stage generic scenario for GRBs. First, a compact source releases about 10^{52} erg, in a small volume of space and on a short time scale. This large concentration of energy expands due to its own pressure. If the rest mass that contaminates the site is not too large, $\leq 10^{-5} M_\odot$, this will result in relativistic expansion with $\gamma > 100$. Finally, at a large enough radius, the kinetic energy (bulk motion) of the expanding material is converted to internal energy and radiated,

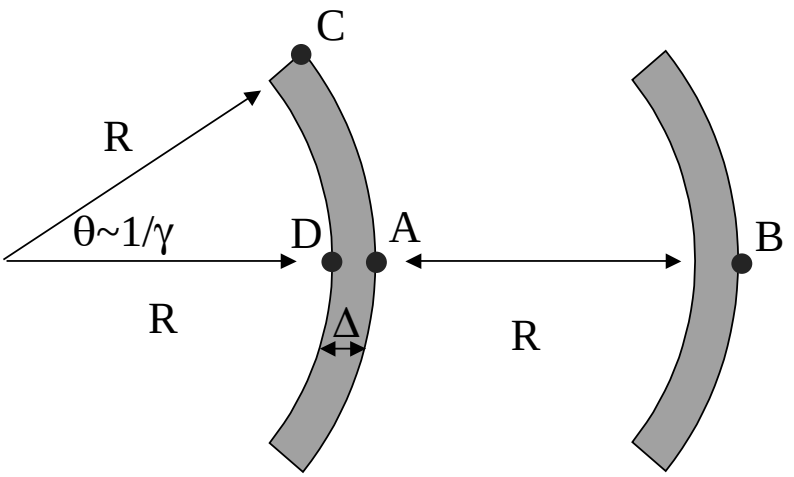

FIGURE 1. Timescales from an expanding relativistic fireball. The gray area represents the observed section of the fireball that can be seen by an observer located far to the right. The angular opening of that section is $1/\gamma$ due to relativistic beaming. Consider the 4 photons emitted at points A, B, C, and D. Photons A, C and D where emitted simultaneously, but photon A will arrive at the observer first, since it is closer to the observer. The arrival-time delay of photons C and D with respect to photon A is simply given by the extra distance they have to travel. Therefore $\delta T_{C-A} = R(1-\cos\theta)/c = R/2\gamma^2 c$, and $\delta T_{D-A} = \Delta/c \sim R/\gamma^2 c$, where we have used the fact that relativistic dynamics of fireballs imply $\Delta \sim R/\gamma^2$. Finally, photon B was emitted long after photon A (about a time R/c later than photon A), however, it is much closer to the observer, resulting in $\delta T_{B-A} = R/2\gamma^2 c$. All three timescales lead to the expression $R/\gamma^2 c$. A short observed variability time scale can therefore be obtained even for large radius, if the Lorentz factor is sufficiently high. The naive estimate of $R \leq c\delta T$ is, therefore, to be replaced by $R \leq \gamma^2 c\delta T$.

mainly in γ-rays. At this stage the system is optically thin and high energy photons can escape. We now discuss this third stage in some detail.

The Arguments For Internal Shocks

Assume a flow carries 10^{52} erg as kinetic energy. In order for this to produce photons, the kinetic energy must be converted back into internal energy and radiated away. The flow must therefore, at least partially, slow down. Two scenarios were proposed for this deceleration: external shocks (Mészáros & Rees 1993) and internal shocks (Narayan, Paczyński, & Piran 1992; Rees & Mészáros 1994). In the external shocks scenario, the relativistic material is running into some (external) ambient medium, possibly the interstellar medium (ISM) or a stellar wind that was emitted earlier by the progenitor. In the internal shocks scenario the inner engine is assumed to emit an irregular flow, that consists of many shells, that travel with a variety of Lorentz factors and therefore collide with one another and thermalize part of their kinetic energy.

The variability observed in many of the bursts was instrumental in constraining

these two possibilities. In the external shocks scenario, this variability is attributed to irregularities in the surrounding medium, e.g., clouds. Each time the ejecta runs into a higher density environment, it produces a peak in the emission. In the internal shocks scenario, the source has to emit many shells, and when two of them collide a peak in the emission is produced. External shocks thus require a complicated surrounding with a relatively simple source that explodes once, while internal shocks require a more complicated source that will explode many times to produce several shells. Due to these very different requirements on the source, the question of internal or external shocks is of a fundamental importance in understanding the nature of the phenomenon.

The size of the clouds that the ejecta runs into, in the external shocks scenario, has to be very small in order to produce peaks that are narrower than the duration of the burst (Fenimore, Madras, & Nayakchin 1996). Sari & Piran (1997a) gave the following argument. The size of the clouds has to be smaller than $R/N\gamma$ to produce peaks that are narrower by a factor of N than the duration of the burst. The number of clouds should be smaller than N otherwise pulses arriving from different clouds will overlap and the amplitude of the variability will be reduced. Finally, the observable area of the ejecta, due to relativistic beaming, is $(R/\gamma)^2$. The maximal efficiency of the external shocks scenario is therefore given by

$$\frac{\text{cloud area} \times \text{number of clouds}}{\text{observed shell area}} \leq \frac{1}{N} \sim 1\%. \qquad (1)$$

Since in many bursts $N > 100$, external shocks have a severe efficiency problem in producing highly variable bursts. Other predictions of external shocks are also inconsistent with the observed temporal profile (Ramirez-Ruiz & Fenimore 1999). Moreover, the density ratio between the clouds and the surroundings has to be huge, of the order of $\gamma N^2 \sim 10^6$, in order for the ejecta to be slowed down mainly by the dense clouds rather than by the low density medium that they are embedded in.

Internal shocks do not suffer from these problems. Detailed calculations show that the observed temporal structure from internal shocks, closely follows the operation of the inner engine that generated the shells (Kobayashi, Piran, & Sari 1997). In this scenario, the source must be variable on time scales shorter than a second and last for as long as 100 seconds, just as the bursts themselves.

The efficiency of internal shocks is largely determined by the ratio of Lorentz factors between different shells which are colliding with each other. The larger the ratio, the larger the efficiency. A simple scenario that demonstrates this is the case of two equal mass shells with Lorentz factor $\gamma_1 \gg \gamma_2 \gg 1$. Conservation of energy and momentum in a collision between the shells leads to a Lorentz factor which is the geometric mean of the initial ones $\sqrt{\gamma_1\gamma_2}$. Therefore, the energy left in the system as non thermal is a small fraction $\sqrt{\gamma_2/\gamma_1} \ll 1$ of the initial energy. Beloboradov (2000) has argued that if large Lorentz factor ratios are allowed, the internal shock efficiency is only limited by the fraction of energy in the shock given to the radiating electrons. Kobayashi & Sari (2001) have then shown that multiple collisions between shocks may result in 'ultra efficient' internal shocks, in the sense that even more than the fraction of energy given to electrons can be radiated away.

The mechanism by which the thermal energy produced by internal shocks is converted to radiation is almost certainly synchrotron and inverse Compton, since these are

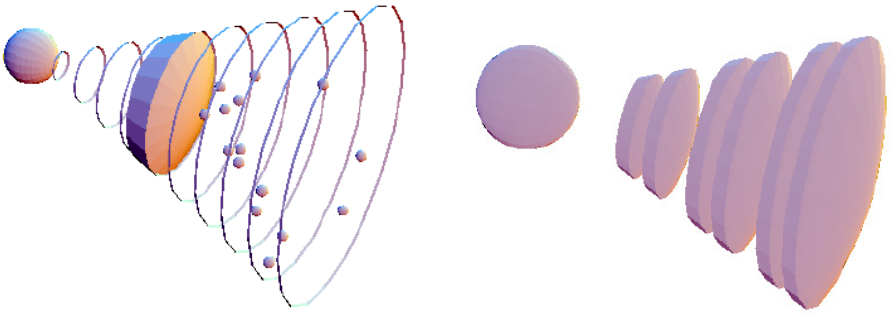

FIGURE 2. Producing variability by external shocks (left) or internal shocks (right). In the external shocks scenario, the variability is produced by irregularities in the surrounding. If the surrounding consists of a low density medium that contains high density clouds, then whenever the shell hits one of the clouds a peak in the emission is produced. The number of clouds, within the observable cone (of angular size $1/\gamma$ due to relativistic beaming) should therefore roughly be the number of observed peaks. The source itself, in this model, needs to produce only a single shell in a single (simple) explosion. However, the external shocks scenario has low efficiency, due to the small total surface area of the clouds when compared to the area of the shell. In the internal shocks case, the temporal structure arises from the source, i.e., the source produces a more complex explosion. There is no efficiency problem, provided that the relative Lorentz factor between shells is large.

the dominant radiation mechanisms at the low densities involved. While both mechanisms probably take place, it is actually not very clear which of the two produces the observed $\sim$ 100keV radiation. Synchrotron emission is for several reasons preferred (Sari, Narayan, & Piran 1996; Sari & Piran 1997b) and inverse Compton probably produces a higher energy component.

THE AFTERGLOW: THEORY AND OBSERVATIONS

After the internal shocks produced the GRB, the shell interacts with the surrounding medium and decelerates. Again it emits radiation by synchrotron and inverse Compton. As the flow decelerates, the emission shifts to lower and lower frequencies. This emission, the afterglow, may last on detectable levels for years after the GRB event!

Afterglow was predicted well before it was observed (Paczyński & Rhoads 1993; Katz 1994; Vietri 1997; Mészáros & Rees 1997). The afterglow theory is relatively simple. It deals with the emission on timescales much longer than that of the GRB. The details of the complex initial conditions are therefore forgotten and the condition of the GRB remnant can be described by a self similar solution with a small number of parameters, such as the total energy and the external density. It is assumed that the electrons are accelerated by the shock into a power-law distribution (index p) of electron Lorentz factors $N(\gamma_e) \propto \gamma_e^{-p}$ for $\gamma_e > \gamma_m$. The lower cutoff, γ_m, of this distribution is set by the assumption that the electrons acquire a fixed fraction, ε_e, of the thermal energy (assumption of equipartition). It is also assumed that a considerable magnetic field is built behind the shock, which is again characterized by a certain fraction ε_B

of equipartition. The energy density behind a relativistic shock is given by $4\gamma^2 n_1 m_p c^2$, where n_1 is the proton density ahead of the shock in units of cm^{-3}, γ is the Lorentz factor of the fluid behind the shock, and m_p is the proton mass. These equipartition assumptions then result in

$$\gamma_m = \frac{p-2}{p-1}\frac{m_p}{m_e}\varepsilon_e\gamma \cong 630\varepsilon_e\gamma \tag{2}$$

$$B = 0.4\sqrt{\varepsilon_B n_1}\gamma \text{ Gauss}, \tag{3}$$

where B is the magnetic field, and m_e is the electron mass. The relativistic electrons then emit synchrotron radiation which produces the observed afterglow. The broad band spectrum of such afterglow emission was given by Sari, Piran, & Narayan (1998).

The afterglow synchrotron spectrum can be described by the electron energy index p, the peak flux, F_m, and three characteristic frequencies (ν_m, ν_c, ν_a):

(I) ν_m is the synchrotron frequency of the minimal energy electron, with Lorentz factor γ_m. From synchrotron theory $\nu_m \cong (eB/2\pi m_e c)\gamma_m^2$ in the local frame of the fluid; here e is the electron charge. Transforming this to the observer frame (blue shifted by the Lorentz factor and redshifted by a factor of $[1+z]$) and using equations (2) and (3) we obtain

$$\nu_m = 1.4\times 10^{13}\text{Hz}\,(1+z)^{-1}\left(\frac{\varepsilon_e}{0.1}\right)^2\left(\frac{\varepsilon_B}{0.1}\right)^{1/2}(\frac{\gamma}{10})^4 n_1^{1/2}. \tag{4}$$

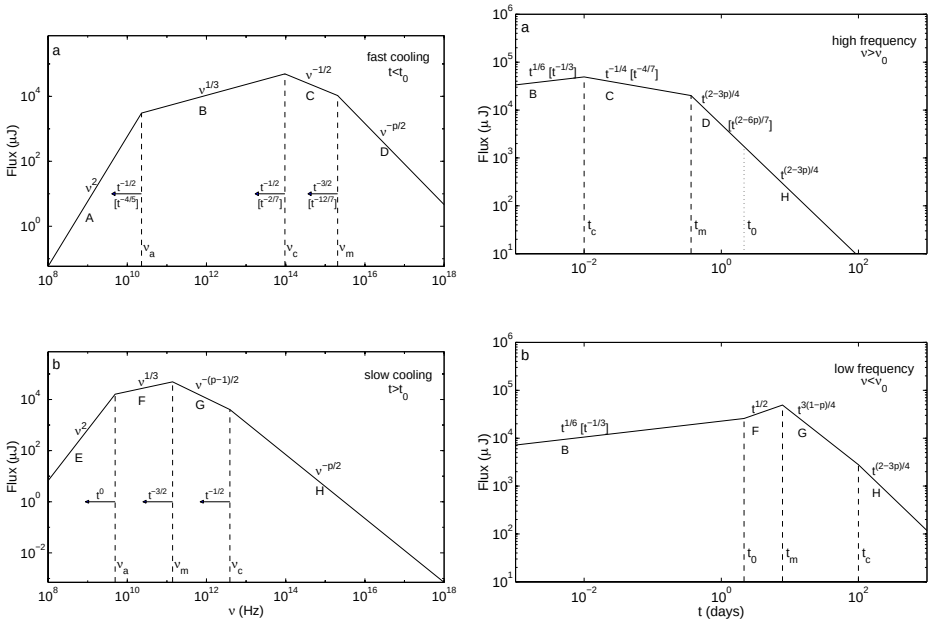

FIGURE 3. Theoretical spectra (left) and light curves (right) of synchrotron emission from a powerlaw distribution of electrons for the case of a constant density ambient medium and a spherical explosion. For most cases $p = 2.2 - 2.5$ fits well the observed spectra and lightcurves.

(II) The cooling time of an electron is inversely proportional to its Lorentz factor γ_e. Therefore, electrons with a Lorentz factor higher than a critical Lorentz factor $\gamma_e > \gamma_c$ cool on the dynamical timescale of the system. This characteristic Lorentz factor is given by the condition $\sigma_T c\gamma^2\gamma_c^2 B^2 t\gamma/6\pi(1+z) = \gamma_c m_e c^2$, and corresponds to the 'cooling frequency'

$$\nu_c = 1.2\times 10^{13}\mathrm{Hz}\,(1+z)\left(\frac{\varepsilon_B}{0.1}\right)^{-3/2}\left(\frac{\gamma}{10}\right)^{-4} n_1^{-3/2} t_{days}^{-2}, \tag{5}$$

where t_{days} is the observer time in days. Here we had also to take into account that time is redshifted.

(III) Below some critical frequency, ν_a, the flux is self-absorbed and is given by the Rayleigh-Jeans portion of a black body spectrum[1]. The self-absorption frequency is given by

$$\nu_{sa} = 93\,\mathrm{GHz}\,(1+z)^{-13/5}\left(\frac{\varepsilon_B}{0.1}\right)^{6/5}\left(\frac{\gamma}{10}\right)^{28/5} n_1^{9/5} t_{days}^{8/5}, \tag{6}$$

if $\nu_c < \nu_m$, and by

$$\nu_{sa} = 87\,\mathrm{GHz}\,(1+z)^{-8/5}\left(\frac{\varepsilon_e}{0.1}\right)^{-1}\left(\frac{\varepsilon_B}{0.1}\right)^{1/5}\left(\frac{\gamma}{10}\right)^{8/5} n_1^{4/5} t_{days}^{3/5}, \tag{7}$$

if $\nu_c > \nu_m$.

(IV) The normalization of the spectrum is given by the total number of radiating electrons $4\pi R^3 n_1/3$ times the peak flux from a single electron, resulting in

$$F_m = 220\,\mathrm{mJy}(1+z)^{-2} d_{L,28}^{-2}\left(\frac{\varepsilon_B}{0.1}\right)^{1/2}\left(\frac{\gamma}{10}\right)^{8} n_1^{3/2} t_{days}^{3}, \tag{8}$$

where $d_{L,28}$ is the luminosity distance in units of 10^{28}cm.

The broad band spectrum of the well-studied GRB 970508 (Galama et al. 1998b) is in good agreement with the theoretical picture. Note that the derivation above is quite general. It does not depend either on the surrounding density profile or on the geometry of the event. Both these effects are hidden in the evolution of the fluid Lorentz factor γ, and the particle density n_1 as a function of time.

The evolution of this spectrum as a function of time depends on the hydrodynamics. The simplest, which describes the observations in some cases quite well, is the adiabatic model with a constant density surrounding medium. The rest mass collected by the shock at radius R is about $R^3\rho$, where ρ is the mass density. On average, the particles move with a Lorentz factor of γ^2 in the observer frame (one factor of γ is the bulk motion and the other is the random thermal motion). Therefore, the total energy is given by $E \propto \gamma^2 R^3 \rho c^2$. Assuming that the radiated energy is negligible compared to the energy of the flow, we obtain that $\gamma \propto R^{-3/2}$ or in terms of the observer time, $t = R/\gamma^2 c$, we get $\gamma \propto t^{-3/8}$. Thus

[1] Granot, Piran, & Sari (2000b) have found that if $\nu_c < \nu_m$, then the self-absorption frequency actually splits into two: ν_{ac} and ν_{sa}, where an optical depth of unity is produced by non-cooled electrons and all electrons, respectively. In between these two frequencies the spectral slope is $\nu^{11/8}$.

$$\nu_m = 6\times10^{15}\,\mathrm{Hz}\,(1+z)^{1/2}E_{52}^{1/2}\varepsilon_e^2\varepsilon_B^{1/2}t_{\mathrm{days}}^{-3/2}$$

$$\nu_c = 9\times10^{12}\,\mathrm{Hz}\,(1+z)^{-1/2}\varepsilon_B^{-3/2}n_1^{-1}E_{52}^{-1/2}t_{\mathrm{days}}^{-1/2}$$

$$\nu_{sa} = 2\times10^{9}\,\mathrm{Hz}\,(1+z)^{-1}\varepsilon_e^{-1}\varepsilon_B^{1/5}n_1^{3/5}E_{52}^{1/5}$$

$$F_m = 20\,\mathrm{mJy}\,(1+z)\varepsilon_B^{1/2}n_1^{1/2}E_{52}d_{L28}^{-2}.$$

These simple scalings, for the case of a constant density ambient medium, lead to the spectral evolution as given in Figure 3. The derivations above use a very simple description of the flow. It represents the fluid as if it has a single magnetic field strength and a single Lorentz factor γ and all of the material is moving directly towards the observer. Also, a very approximate description of the synchrotron emission was used. In reality, of course, the situation is more complicated. There are two effects that must be taken into account. The most dramatic one is the fact that matter slightly off the line of sight does not move directly towards the observer (Waxman 1997b; Panaitescu & Mészáros 1998; Sari 1998). The amount of Lorentz boost from that matter is reduced. Secondly, fluid elements at different distances from the shock have somewhat different Lorentz factors, magnetic fields and electron energies. These variations can be estimated using the self-similar solution of Blandford & McKee (1976). The outcome of these more detailed calculations are the same scaling laws, but with a more accurate coefficient for the break frequencies as well as an estimate of the shape of the spectrum around each break frequency (Granot, Piran, & Sari 2000a; Gruzinov & Waxman 1999; Granot, Piran, & Sari 1999; Granot & Sari 2002). The equations given above already take these effects into account, and the coefficients given are accurate for $p = 2.2$.

Given the above hydrodynamic evolution, one can construct light curves at any given frequency. These will also consist of power laws, changing from one power law to the other once the break frequencies pass through the observed band. These predicted power law lightcurves and spectra are in fair agreement with afterglow observations.

The observational breakthrough came in early 1997, when quick and accurate position of GRBs by BeppoSAX (Jager et al. 1993; Piro, Scarsi, & Butler 1995) led to the discoveries of X-ray (Costa et al. 1997), optical (Van Paradijs et al. 1997), millimeter (Bremer et al. 1998) and radio (Frail et al. 1997) counterparts of GRBs. These observations quickly settled the distance controversy. The first transient optical counterpart, of GRB 970228, is in a faint galaxy with $\sim 0.8''$ diameter (Sahu et al. 1997). Several authors (Wijers, Rees, & Mészáros 1997; Reichart 1997; Waxman 1997a) showed that to first order this model describes the X-ray and optical afterglow of GRB 970228 very well. The detection of absorption features in the OT's spectrum of GRB 970508 (Metzger et al. 1997) established that this event was at a redshift greater than $z = 0.835$. GRBs come from 'cosmological' distances and are thus extremely powerful events. They are by far the most luminous photon sources in the Universe, with (isotropic equivalent) peak luminosities in γ-rays up to 10^{52} erg/s, and total energy budgets (assuming isotropy) up to several 10^{53-54} erg (Kulkarni et al. 1998a, 1999b). Within the first day, the optical emission is usually brighter than 20th magnitude and therefore small telescopes can play an

important role in measuring the lightcurve. Nowadays, a large worldwide collaboration is observing these events and the data are submitted to a Global-Coordinate-Network in real time, allowing other observatories to react rapidly.

GRB 970508 was the first GRB with a radio counterpart (Frail et al. 1997). The radio light curves (8.5 and 4.9 GHz) show large variations on time scales of less than a day, but these damp out after one month. This finds a viable explanation in interstellar scintillation (irregular plasma refraction by the interstellar medium between the source and the observer). The damping of the fluctuations can then be understood as the effect of source expansion on the diffractive interstellar scintillation. Thus a source size of roughly 10^{17} cm was derived (at 3 weeks), corresponding to a mildly relativistic expansion of the shell (Frail et al. 1997).

GRB 970508 remains one of the best observed afterglows: the radio afterglow was visible at least 400 days (Frail, Waxman, & Kulkarni 2000), and the optical afterglow up to $\sim$ 450 days (e.g., Fruchter et al. 2000; Galama et al. 1998a; Castro-Tirado et al. 1998). In addition to millimeter (Bremer et al. 1998), infrared and X-ray (Piro et al. 1998) counterparts were detected, and it is the first GRB for which a spectral transition in the optical/near IR range was found (Galama et al. 1998b,a); this transition is interpreted as the effect of the passage of the cooling frequency through the optical/near IR passbands. These multi-wavelength observations allowed the reconstruction of the broad radio to X-ray spectrum for this GRB (Galama et al. 1998b) (see Figure 4). Galama et al. (1998b) found that the 'standard' model provides a successful and consistent description of the afterglow observations over nine decades in frequency, ranging in time from the event until several months later. The synchrotron afterglow spectrum of this GRB allows measurement of the electron energy spectrum slope, p, the three break frequencies (ν_a, ν_m and ν_c), and the flux at the peak, F_m. For GRB 970508 the redshift, z, is also known, and all blast wave parameters could be deduced: the total energy (per unit solid angle) E = 3.5×10^{52} erg, the ambient (nucleon) density $n_1 = 0.030$, the fraction of the energy in electrons $\varepsilon_e = 0.12$ and that of the magnetic field $\varepsilon_B = 0.089$ (Wijers & Galama 1999). The numbers themselves are uncertain by an order of magnitude (see, e.g., Granot, Piran, & Sari 1999), but the result shows that the 'standard' model fits the expectations very well. Following these first attempts at modeling the broad-band afterglow, more detailed modeling efforts have been made on other well-studied afterglows (Berger et al. 2000; Panaitescu & Kumar 2001, 2002; Panaitescu 2001; Harrison et al. 2001; Yost et al. 2002; Frail et al. 2003; Yost et al. 2003).

COLLIMATED OUTFLOW - JETS

The hydrodynamic evolution described in the previous section assumed spherical symmetry. However, many astrophysical phenomena, especially those involving extreme energetics are not spherical but in the form of jets. This is most probably the case also for GRBs.

Jets have been discussed extensively in the context of GRBs. First, the similarity between some of the observed features of blazars and AGNs led to the speculation that jets also appear in GRBs (Paczyński 1993). Second, the regions emitting the GRBs as well as the afterglow must be moving relativistically. The emitted radiation is strongly

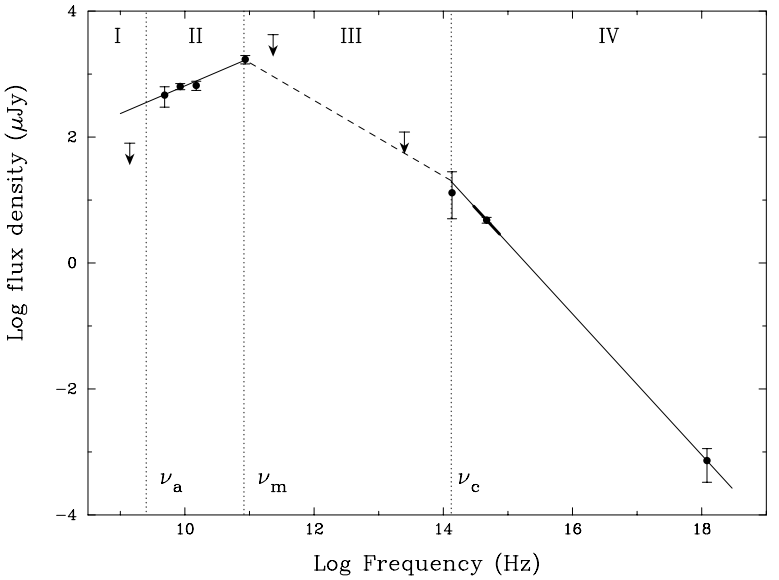

FIGURE 4. The X-ray to radio spectrum of GRB 970508 on May 21.0 UT (12.1 days after the event). The location of the break frequencies ν_a, ν_m and ν_c, inferred from transitions in the light curves and from spectra of the afterglow, are indicated (from Galama et al. 1998b).

beamed, and we can observe only a region with an opening angle $1/\gamma$ off the line of sight. Emission outside of this very narrow cone is not observed. These considerations have lead to numerous speculations on the existence of jets and to attempts to search for the observational signature of jets both during the GRB phase (Mao & Yi 1994) and in the context of the afterglow (Rhoads 1997, 1999; Mészáros, Rees, & Wijers 1998). Finally, jets appear naturally in the context of several leading scenarios for the 'inner engine'.

We begin by clarifying some of the confusing terminology. There are two distinct, but related, effects. The first, *'jets'*, describes scenarios in which the relativistic flow emitted from the source is not isotropic but collimated towards a finite solid angle. The term jet refers to the geometrical shape of the relativistic flow emitted from the inner engine. The second effect is that of *'relativistic beaming'*. The radiation from any object that is radiating isotropically in its own rest frame, but moving with a large Lorentz factor γ in the observer frame, is beamed into a small angle $1/\gamma$ around its direction of motion. This is an effect of special relativity. It has nothing to do with the ejecta's geometry (spherical or jet) but only with the fact that the ejecta is moving relativistically. The effect of relativistic beaming allows an observer to see only a small angular extent, of size $1/\gamma$ centered around the line of sight. Since we know the flow is ultra-relativistic (initially $\gamma > 100$), there is no question that the relativistic beaming effect is always relevant for GRBs. The question we are interested in is that of the existence of 'jets'.

The idealized description of a jet is a flow that occupies only a conical volume with half opening angle θ_0. In fact, the relativistic dynamics is such that the width of the

material in the direction of its propagation is much smaller than its distance from the source by a factor of $1/\gamma^2$. The flow, therefore, does not fill the whole cone. Instead it occupies only a thin disk at its base, looking more like a flying pancake (Piran 1999) (see Figure 2). If the 'inner engine' emits two such jets in opposite directions then the total solid angle towards which the flow is emitted is $\Omega = 2\pi\theta_0^2$. Whether the relativistic flow is in the form of a jet or a sphere has two important implications:

The Total Emitted Energy. Optical observations of afterglows enabled redshift determination, and therefore a reasonably accurate estimate of the distance, D, to these events (the uncertainty is now in the cosmological parameters of the Universe). The so called 'isotropic energy' can then be inferred from the fluence F (the total observed energy per unit area at earth) as $E_{iso} = 4\pi D^2 F$ (taking cosmological corrections into account, $D = d_L/\sqrt{1+z}$ where d_L is the luminosity distance and z is the redshift). The numbers obtained in this way range from 10^{51} erg to 10^{54} erg with the record of 3×10^{54} erg held by the famous GRB 990123. These huge numbers approach the equivalent energy of a solar mass, all emitted in a few tens of seconds! If instead the emission is confined to some solid angle Ω then the true energy is $E = \Omega D^2 F$.

The Event Rate. BATSE's detection rate of about one burst per day, combined with several redshift measurements, translates to about 10^{-7} bursts per year per galaxy or 0.5 bursts/Gpc^{-3}/year (Schmidt 1999, 2001; Perna, Sari, & Frail 2003). However, if the emission is collimated to $\Omega \ll 4\pi$ then we do not see most of the events. The true event rate is then larger than that measured by BATSE by a factor of $4\pi/\Omega$ (see, however, Perna, Sari, & Frail 2003).

The Jet-break

As the afterglow evolves, γ decreases and it will eventually fall below the initial inverse opening angle of the jet. The observer will notice that some of the sphere is missing from the fact that less radiation is observed. This effect alone, will produce a significant break, steepening the lightcurve decay by a factor of $\gamma^2 \propto t^{-3/4}$ even if the dynamics of each fluid element has not changed. The transition should occur at the time t_{jet} when $1/\gamma \cong \theta_0$. Observing this time can therefore provide an estimate of the jet's opening angle according to

$$t_{\rm jet} \approx 6.2{\rm hr}(1+z)(E_{52}/n_1)^{1/3}(\theta_0/0.1)^{8/3}. \qquad (9)$$

Additionally, Rhoads (1999) has shown that at about the same time (see, however, Panaitescu & Mészáros 1999; Mészáros & Rees 1999a; Moderski, Sikora, & Bulik 2000; Granot et al. 2001), the jet will begin to spread laterally so that its opening angle $\theta(\hat{t}) \sim 1/\gamma$. The ejecta now encounters more surrounding matter and decelerates faster than in the spherical case. The Lorentz factor then decays exponentially with the radius and as $\gamma \propto t^{-1/2}$ with observed time. Taking this into account, the observed break is even more significant. The slow cooling spectrum given in Figure 3 evolves with decreasing peak flux $F_m \propto t^{-1}$ and the break frequencies evolve as $\nu_m \propto t^{-2}$, $\nu_c \propto t^0$ and $\nu_a \propto t^{-1/5}$. This translates to a temporal decay in a given frequency as listed in Table 1. The jet break

is a hydrodynamic one. It should therefore appear at the same time at all frequencies - an achromatic break[2].

TABLE 1. The spectral index β and the temporal index α as function of p for a spherical and a jet-like evolution. Typical values are quoted using $p = 2.4$. The parameter free relation between α and β is given for each case (eliminating p). The difference in α between a jet and a sphere is always substantial at all frequencies.

	spectral index β, $F_\nu \propto \nu^{-\beta}$	light curve index α, $F_\nu \propto t^{-\alpha}$ sphere	jet
$\nu < \nu_a$	$\beta = -2$	$\alpha = -1/2$	$\alpha = 0$
$\nu_a < \nu < \nu_m$	$\beta = -1/3$	$\alpha = -1/2$	$\alpha = 1/3$
$\nu_m < \nu < \nu_c$	$(p-1)/2 \cong 0.7$	$\alpha = 3(p-1)/4 \cong 1.05$ $\alpha = 3\beta/2$	$\alpha = p \cong 2.4$ $\alpha = 2\beta + 1$
$\nu > \nu_c$	$p/2 \cong 1.2$	$\alpha = (3p-2)/4 \cong 1.3$ $\alpha = 3\beta/2 - 1/2$	$\alpha = p \cong 2.4$ $\alpha = 2\beta$

The theory of jet evolution and of the resulting light curves had been worked out before evidence for jets was obtained. In fact, Rhoads (1999), has used this theory to constrain the amount of collimation in GRB 970508, which did not show any significant steepening of the afterglow lightcurve. He concluded that the opening angle of a jet, if it exists, must be more than 30 degrees.

The first claims for narrow jets came from GRB 990123 (Kulkarni et al. 1999b; Castro-Tirado et al. 1999; Fruchter et al. 1999) and from analysis of a few fast decaying afterglows (Sari, Piran, & Halpern 1999). The latter noted that the observed decays in GRB afterglows that do not show a break are either of a shallow slope, $F_\nu \propto t^{-1.2}$, or a very steep slope, $F_\nu \propto t^{-2}$. They argued that the rapidly decaying bursts are those in which the ejecta was a narrow jet and the break in the light curve was before the first observations. Interestingly, evidence for jets are found when the inferred energy (without taking jets into account) is the largest. This implies that the jets account for a considerable fraction of the wide luminosity distribution seen in GRBs, and the true energy distribution is less wide than it seems to be.

A similar transition was better sampled in afterglow data of GRB 990510 (see Figure 5); optical observations of GRB 990510, show a clear steepening of the rate of decay of the light simultaneously in all optical bands between $\sim$ 3 hours and several days (Harrison et al. 1999; Stanek et al. 1999) to roughly $F_\nu(t) \propto t^{-2.2}$. Together with radio observations, which also reveal a transition, it is found that the transition is very much frequency-independent; this virtually excludes explanations in terms of the passage of the cooling frequency, but is what is expected in case of beaming. Harrison et al. (1999) derive a jet opening angle (from the jet-break time) of $\theta_0 \cong 0.08$, which for this burst would reduce the total energy in γ-rays to $\sim 10^{51}$ erg.

[2] Sari (1997), argued that there may be about a factor of two difference in the effective transition time between the four different spectral regimes (e.g., below or above ν_m) due to the fact that the emission in these different regimes weighs differently contributions from various emission radii.

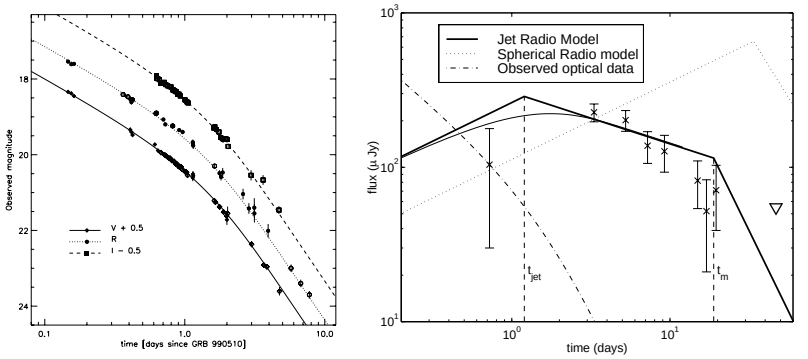

FIGURE 5. GRB 990510, the 'classical' case for a 'jet': an achromatic break in optical and radio at $t_{\rm jet} = 1.2$ days implying a jet-opening angle $\theta_0 = 0.08$. The temporal slope before and after the break agree well with the theory if $p = 2.2$. For this burst the isotropic γ-ray energy $E_{\rm iso} = 2.9 \times 10^{53}$ erg but the 'true' total energy is only $E = 10^{51}$ erg. From Harrison et al. (1999).

Frail et al. (2001) have determined the jet-break times for a sample of GRBs with known redshifts. From these, a wide range of jet-opening angles is inferred in GRBs: from 3° to more than 25°, with a strong concentration near 4°. This relatively narrow collimation implies that the observed GRB rate has to be corrected for the fact that conical fireballs are visible to only a fraction of observers. Frail et al. find that the 'true' GRB rate is ~ 500 times larger than the observed GRB rate. Although the isotropic equivalent energies of GRBs range from about 5×10^{51} to 1.4×10^{54} erg, when one corrects the observed γ-ray energies for the geometry of the outflow, GRB energies appear narrowly clustered around 5×10^{50} erg (see Figure 6).

The central engines of GRBs thus produce approximately a similar amount of energy, and the broad range of fluence and luminosity observed for GRBs appears largely the result of a wide variation of opening angles. Berger et al. (2003) suggested that the energy in the γ-ray part of the spectrum may fall below the Frail et. al. relation, however, the total energy emitted (some of which may be in more mildly relativistic ejecta) is still constant, and reveals itself during the afterglow stage.

Postnov, Prokhorov, & Lipunov (2001); Rossi, Lazzati, & Rees (2002); Zhang & Mészáros (2002) pointed out that another interpretation is possible for the Frail et. al result. Instead of a variety of jets with different opening angles, a standard jet can be invoked with energy density per unit solid angle falling away from the axis as θ^{-2}; the differences in the apparent opening angle comes from variation in the orientation of the observer relative to the jet's axis. Perna, Sari, & Frail (2003) showed that the distribution of the observed opening angles is consistent with this assumption, adding credence to the universal jet model (see, however, Nakar, Granot, & Gueta 2004). If this model is correct, the rate of GRBs is much lower as it should not be corrected by the factor of 500 of Frail et. al., however, the energy is still low, of order 10^{51} erg. Clearly, additional complication may exist, and the ejecta may be non-uniform on smaller scales, the so-called patchy shell model (Kumar & Piran 2000b) or minijets (Yamazaki, Ioka, & Nakamura 2004).

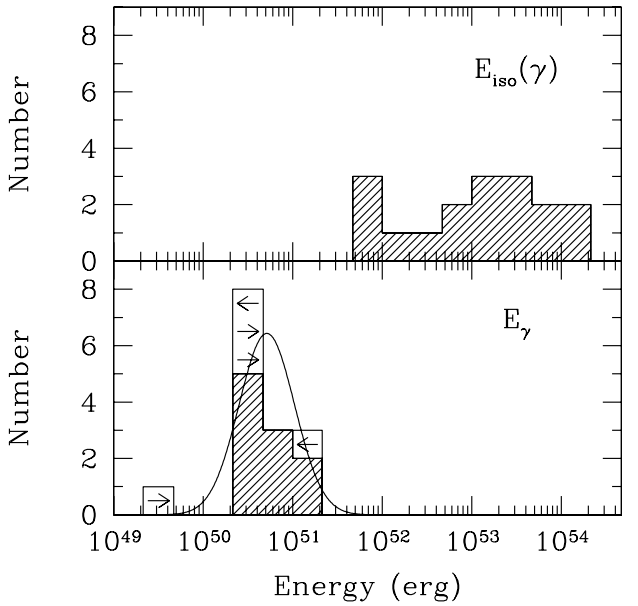

FIGURE 6. The distribution of the apparent isotropic γ-ray burst energy of GRBs with known redshifts (top) versus the geometry-corrected energy (bottom). While the isotropic energy E_{iso} spans three orders of magnitudes, the geometrically corrected energy, $E_\gamma = E_{iso}\theta^2/2$, is very narrowly distributed. This implies that the sources of GRBs produce roughly the same amount of energy, about 5×10^{50}erg, but that energy is distributed over a variety of angles resulting in a wide distribution of isotropic energies. From Frail et al. (2001).

POLARIZATION - A PROMISING TOOL

An exciting possibility to further constrain the models and obtain a more direct proof of the geometrical picture of 'jets' is to measure linear polarization. Varying polarization at optical wavelengths has been observed in GRB afterglows at the level of a few percent (Wijers et al. 1999; Rol et al. 2000).

High levels of linear polarization are usually the smoking gun of synchrotron radiation. The direction of the polarization is perpendicular to the magnetic field and can be as high as 70%. Gruzinov & Waxman (1999) and Medvedev & Loeb (1999) considered the emission from spherical ejecta which by symmetry should produce no polarization on the average, except for fluctuations of order a few percent. Polarization is more natural if the ejecta is a 'jet' and the line of sight to the observer is within the jet but does not coincide with its axis. In this case, the spherical symmetry is broken (Gruzinov 1999; Ghisellini & Lazzati 1999; Sari 1999), and the polarization produced by synchrotron radiation will not vanish. For simplicity, lets assume that the magnetic field behind the shock is directed along the shock's plane (the results hold more generally, as long as the magnetic field has a preferred direction). The synchrotron polarization from each part

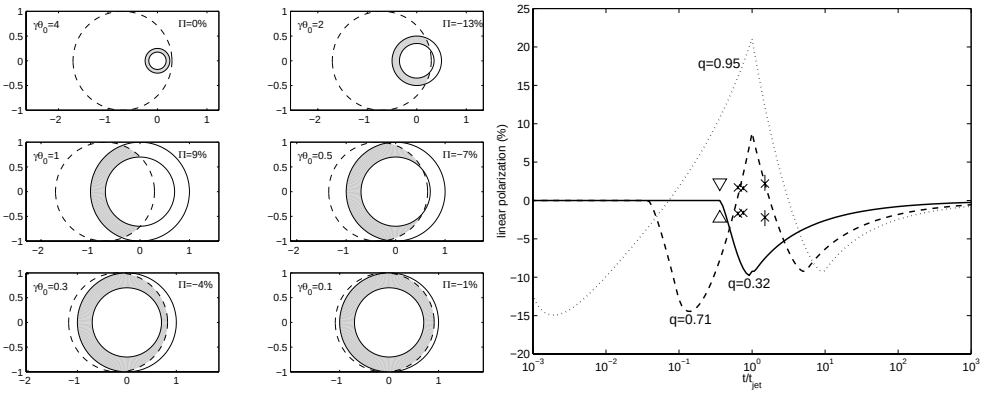

FIGURE 7. Left: Shape of the emitting region. The dashed line marks the physical extent of the jet, and solid lines give the viewable region $1/\gamma$. The observed radiation arises from the gray-shaded region. In each frame, the percentage of polarization is given at the top right and the initial size of the jet relative to $1/\gamma$ is given on the left. The frames are scaled so that the size of the jet is unity. Right: Observed and theoretical polarization lightcurves for three possible offsets of the observer relative to the jet axis Observational data for GRB 990510 is marked by crosses (x), assuming $t_{jet} = 1.2$ days. The upper limit for GRB 990123 is given by a triangle, assuming $t_{jet} = 2.1$ days.

of the shock front, which is perpendicular to the magnetic field, is therefore directed radially.

As long as the relativistic beaming angle $1/\gamma$ is narrower than the physical size of the jet, θ_0, one is able to see a full ring and therefore the radial polarization averages out (the first frame, with $\gamma\theta_0 = 4$ of the left plot in Figure 7). As the flow decelerates, the relativistic beaming angle $1/\gamma$ becomes comparable to θ_0 and only a part of the ring is visible; net polarization is then observed. Note that due to the radial direction of the polarization from each fluid element, the total polarization is maximal when a quarter ($\gamma\theta_0 = 2$ in Figure 7) or when three quarters ($\gamma\theta_0 = 1$ in Figure 7) of the ring are missing (or radiate less efficiently) and vanishes for a full and for half ring. The polarization, when more than half of the ring is missing, is perpendicular to the polarization direction when less than half of it is missing.

At late stages the jet expands sideways and since the offset of the observer from the physical center of the jet is constant, spherical symmetry is regained. The vanishing and re-occurrence of significant parts of the ring results in a unique prediction: there should be three peaks of polarization, with the polarization position angle during the central peak rotated by 90° with respect to the other two peaks. In case the observer is very close to the center, more than half of the ring is always observed, and therefore only a single direction of polarization is expected. A few possible polarization light curves are presented in Figure 7.

Excellent polarization data is available for the bright afterglow of GRB 030329 (Greiner et al. 2003). Unfortunately, this bursts shows considerable variability in its afterglow, that suggest a complex jet structure, and does not allow for a straight forward comparison with the theory. Yet, a few conclusions seems generic. First, the variations

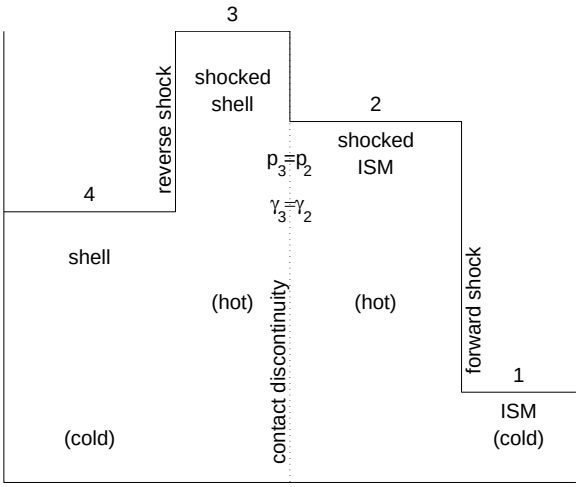

FIGURE 8. Schematic representation of the four zones that are present when a relativistic fireball starts to interact with the interstellar medium (ISM). The solid line indicates the density as a function of radius. The undisturbed ISM is zone 1 at large radius, and the unshocked shell material is zone 4 at small radii. The shocked zones, 2 and 3, are the result of the forward and reverse shocks and are separated by a contact discontinuity (based on Sari & Piran 1995).

of the magnitude of polarization without change in the position angle favor geometrical effect (e.g., Gruzinov 1999; Ghisellini & Lazzati 1999; Sari 1999) rather than that of random magnetic field cells (e.g., Gruzinov & Waxman 1999; Medvedev & Loeb 1999). Second, the low level of polarization suggest that the magnetic field is quite entangled with the components in the two directions differing by about 10%. Third, the erratic polarization behavior seems to support the complex jet structure deduced from the fluctuating optical light curve.

THE REVERSE SHOCK EMISSION

The previous sections discussed the theory and the observations of the 'late' afterglow, hours or more after the burst. During that time, most of the energy of the system was already given to the shocked surroundings, and it is that region that dominates the emission. However, during the first few tens of seconds, the evolution of the Lorentz factor as a function of time is not self similar. There are two shocks: a forward shock going into the surrounding medium and a reverse shock going into the expanding ejecta (see Figure 8). The hydrodynamic details were discussed in Sari & Piran (1995).

During the initial stages, the internal energy stored behind the shocked-surrounding matter and the energy of the shocked ejecta are comparable. However, the temperature of the shocked ejecta is much lower, typically by a factor of $\gamma \sim 10^2$. This results in an additional emission component with a typical frequency lower by a factor of $\gamma^2 \sim 10^4$, which, for typical parameters, is near the optical passband. Contrary to the 'standard'

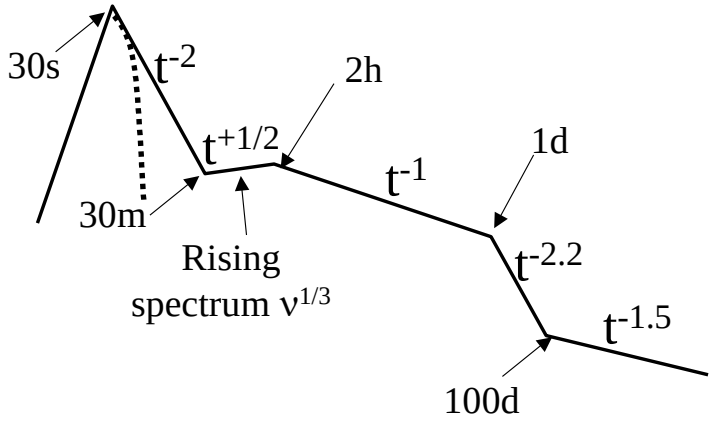

FIGURE 9. Predicted optical afterglow-light curve over more than six orders of magnitude in time (from a few seconds up to a about year). Sequentially from left to right: a rapid rise to maximum emission from the reverse shock, followed by a rapid decay $F \propto t^{-2}$ as the reverse-shock heated ejecta cool down. When the emission from the forward shock takes over, the flux is expected to rise slowly as $F \propto t^{+1/2}$ up to a second peak when the frequency ν_m of the forward shock passes the optical passband. During that rise, a positive spectral slope is expected, which has not yet been observed. The subsequent decay of roughly $F \propto t^{-1}$ is steepened to about $F \propto t^{-2.2}$ due to the jet break. The final transition is to the non-relativistic phase.

late afterglow, this emission is very sensitive to the initial Lorentz factor. Theoretical predictions for such a flash were given in detail by Sari & Piran (1999c,a) and were earlier suggested as a possibility by Mészáros & Rees (1997). Figure 9 is a sketch of the predicted optical lightcurve combining the reverse shock, the forward shock, the jet break and the transition to subrelativistic velocities.

One of the most exciting events in the field of afterglow studies, was the detection of an extremely bright (9th magnitude from $z = 1.6$) optical emission simultaneous with GRB 990123 by the ROTSE team (Akerlof et al. 1999). The ROTSE telescope obtained its first images only 22 seconds after the start of GRB 990123 (i.e., during the GRB), following a notification received from BATSE. The ROTSE observations show that the optical light curve peaked at $m_V \sim 9$ magnitudes some 60 seconds after the event (Akerlof et al. 1999). After maximum a fast decay followed for at least 15 minutes. The late-time afterglow observations show a more gradual decline (Galama et al. 1999; Kulkarni et al. 1999b; Castro-Tirado et al. 1999; Fruchter et al. 1999; Sari & Piran 1999b) (see Figure 10). Galama et al. (1999) have shown, that if one assumes that the emission detected by ROTSE comes from a non-relativistic source of size ct, then the observed brightness temperature $T_b > 10^{17}$ K of the optical flash exceeds the Compton limit of 10^{12} K. This confirms the highly relativistic nature of the GRB source.

The ROTSE observations show that the prompt optical and γ-ray light curves do not track each other (Akerlof et al. 1999). In addition, detailed comparison of the prompt optical emission with the BATSE spectra of GRB 990123 (at three epochs for which both optical and γ-ray information is available) shows that the ROTSE emission is not a

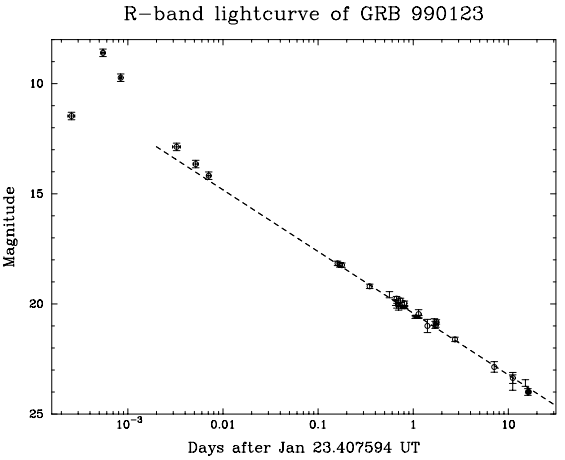

FIGURE 10. R-band light curve of the afterglow of GRB 990123. The ROTSE data show that the optical light curve peaked at $m_V \sim 9$ (Akerlof et al. 1999). The dashed line indicates a power law fit to the light curve (for $t > 0.1$ days), which has exponent -1.12 ± 0.03 (from Galama et al. 1999).

simple extrapolation of the GRB spectrum to much lower energies (Galama et al. 1999; Briggs et al. 1999).

The observed optical properties of this event are well described by emission from the reverse shock that initially decelerates the ejecta, provided that the initial Lorentz factor is about 200 (Sari & Piran 1999b; Mészáros & Rees 1999b). It takes tens of seconds for the reverse shock to sweep through the ejecta and produce the bright flash. Later, the shocked hot matter expands adiabatically and the emission quickly shifts to lower frequencies and considerably weakens.

Another new ingredient that was found in GRB 990123 is a radio flare (Kulkarni et al. 1999a). Contrary to all other afterglows, where the radio peaks around a few weeks and then decays slowly, this burst had a fast rising flare, peaking around a day and then decaying quickly. This can be interpreted as emission from the cooling ejecta that was earlier on heated by the reverse shock. Using the Blandford & McKee (1976) self-similar solution to derive the evolution of the ejecta and its emission properties one finds that the typical frequency scales as $\nu_m^r \propto t^{-73/48}$ and the flux at that frequency scales as $F_m^r \propto t^{-47/48}$ (Sari & Piran 1999a) (see Kobayashi & Sari (2001) for revised scalings when the temperature of the ejecta is non relativistic). Therefore, within a day the emission from the adiabatically cooling ejecta that produced the 60s optical flash in GRB 990123 is expected to shift to radio frequencies (Sari & Piran 1999b). Using the observed optical flash, and the above scalings, a good fit to the radio data is obtained. The optical flash and the radio flare may therefore be related.

Given the above interpretation of the reverse shock emission, it is important to ask whether GRB 990123 is an exception, or whether the phenomena of radio flares and optical flashes is more common. Radio flares appear to exist in other cases (Frail et al. 2001). However, since early radio data is usually sparse, and these events did not have an early optical observation to find the associated optical flash, the interpretation in terms

of emission from the reverse shock is less secure than in the case of GRB 990123. In the optical, from robotic optical experiments such as ROTSE and LOTIS, strong upper limits exists for several bursts. The upper limits show that the optical flash does not scale with the fluence of the event (Akerlof et al. 2000; Kehoe et al. 2001; Rykoff et al. 2004; Quimby et al. 2006; Rykoff et al. 2006). However, with reasonably small changes in the density or the initial Lorentz factor, those events could have escaped detection (Kobayashi 2000; Kobayashi et al. 2005). More detailed work argues that the reverse shock emission was overestimated and suggested more observational tests (Nakar & Piran 2004; Panaitescu & Kumar 2004; Nakar & Piran 2005). Once satellites provide accurate positioning on timescales of seconds, strong constraints on the generality of optical flashes and radio flares will be possible to obtain.

Finally, we mention the possibility of a source operating on an afterglow timescale. In this case the reverse shock continues for a long time, newly shock-heated electrons are continuously created, and the emission in a significant part of the spectrum, especially in the sub-mm regime (Kumar & Piran 2000a; Sari & Mészáros 2000), will be dominated by the reverse shock. A similar situation will occur if the source has emitted a slower, but energetic shell, which later catches up with the decelerating ejecta. The relation between the reverse and forward shock spectrum in such a case was given in Sari & Mészáros (2000).

PROGENITORS

Observationally it is hard to distinguish between models of progenitors for GRBs. The GRB and the afterglow are produced when relativistic ejecta are slowed down, and no observable radiation emerges directly from the 'hidden engine' that powers the GRB. Thus, despite all discoveries the origin of GRBs has remained rather mysterious for a long time. Popular models for the origin of GRBs that (in principle) can provide the required energies, come in two classes: (i) compact object mergers such as the neutron star-neutron star (e.g., Eichler et al. 1989) and neutron star-black hole mergers (Narayan, Paczyński, & Piran 1992; Mochkovitch et al. 1993; Lattimer & Schramm 1974), and (ii) the core collapses of very massive stars (termed collapsars, 'failed' supernovae, or hypernovae (Woosley 1993; Paczyński 1998; MacFadyen & Woosley 1999)). In both cases (Iwamoto et al. 1998; Woosley, Eastman, & Schmidt 1999) a solar mass black hole is formed with an accretion disk around it. Simply based on accretion timescales, one may suspect that the neutron star mergers would be short events, while collapse of massive stars produce accretion disks which survive for longer (Narayan et al. 2001).

The first observational evidence for a possible GRB/SN connection was provided by the discovery of SN 1998bw in the error box of GRB 980425 (Galama et al. 1998c). Their temporal and spatial coincidence suggested that the two phenomena are related (Galama et al. 1998c; Kulkarni et al. 1998b). In addition, the radio emitting shell in SN 1998bw must be expanding at relativistic velocities, $\gamma > 2$ (Kulkarni et al. 1998b). This had thus far never been observed in a SN. From minimum energy arguments, it was estimated that this relativistic shock carried 5×10^{49} erg, and could well have produced the GRB at early time (Tan, Matzner, & McKee 2001; Chevalier & Li 1999).

The total γ-ray energy budget of GRB 980425 is about a factor of $\sim 10^5$ smaller than

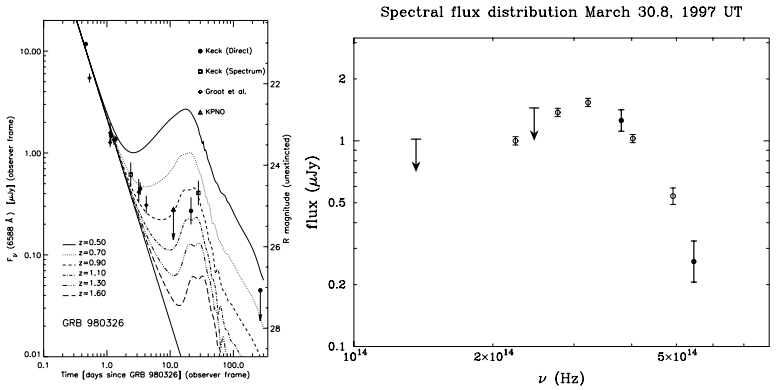

FIGURE 11. Left: R-band light curve of GRB 980326 and the sum of an initial power-law decay plus Ic supernova light curve for redshifts ranging from $z = 0.50$ to $z = 1.60$ (from Bloom et al. 1999). Right: The broad-band spectrum of the OT of GRB 970228 at March 30.8, 1997 UT (• and upper-limit arrow). Also shown is the spectral flux distribution of SN 1998bw (○) redshifted to the redshift of GRB 970228 ($z = 0.695$). The similarity of the spectral flux distributions is remarkable (from Galama et al. 2000).

those of 'normal' GRBs (Galama et al. 1998c). Evidence for a possible supernova connection for the 'normal' high-luminosity GRBs comes from the late-time red spectrum and the late-time rebrightening of their afterglow light curves. GRB 980326 shows possible evidence that at late times the emission is dominated by an underlying supernova (Bloom et al. 1999). A template supernova light curve, provided by the well-studied type $I_{b/c}$ SN 1998bw provides an adequate description of the observations (see Figure 11). Similar evidence where later found in other GRBs (Reichart 1999; Galama et al. 2000).

The ultimate evidence for the GRB/SN connection came with the observation of GRB 030329. This burst was relatively nearby allowing accurate spectra at the time of the expected SN peak. Indeed, as the afterglow decayed, a spectrum remarkably close to that of SN1998bw was revealed (Stanek et al. 2003; Kawabata et al. 2003; Matheson et al. 2003; Mazzali et al. 2003). Large observational campaign of this bright nearby event (Sheth et al. 2003; Burenin et al. 2003; Tiengo et al. 2003; Smith et al. 2003; Torii et al. 2003; Urata et al. 2004; Lipkin et al. 2004; Frail et al. 2005) allowed direct measure of its afterglow size (Taylor et al. 2004) in agreement with theoretical models (Taylor et al. 2004; Granot et al. 2005). Given this identification, it is now clear that the interpretation of red bumps in several afterglows as signals of SN was justified. Two more cases of clear supernovae spectra followed GRB 031203 (Malesani et al. 2004; Soderberg et al. 2004; Watson et al. 2004; Thomsen et al. 2004; Gal-Yam et al. 2004) and GRB 060218 (Modjaz et al. 2006; Mirabel et al. 2006; Sollerman et al. 2006; Soderberg et al. 2006). It is now clear that a significant fraction of long GRBs are accompanied by SN.

Short GRBs

The understanding of the progenitor of short GRBs is advancing rapidly these days due to recent prompt localizations by both HETE-II and SWIFT that lead to detection of afterglows (Gherels et al. 2005; Bloom et al. 2006; Fox et al. 2005; Hjorth et al. 2005a; Covino et al. 2006; Berger et al. 2005; Hjorth et al. 2005b; Villasenor et al. 2005). It is already clear that many of them are not associated with supernovae. They form then at least one new class of progenitors. It is becoming clear that these progenitors are more long-lived as they are not located in star forming regions or even star forming galaxies. Some of them seem to be located in low density environments. Neutron star mergers seems compatible with these findings and is perhaps the leading candidate for the progenitor of short GRBs. This already prompts renewed estimates of lifetimes of double neutron star systems and comparison with the observed redshift distributions (Nakar et al. 2006; Nakar, Gal-Yam, & Fox 2006; Belczynski et al. 2006). The detection of an extremely bright giant flare from SGR 1906-20 raised for a while the possibility that a significant fraction of short GRBs are actually giant flares of magnetars in nearby galaxies. Though the physics of those events may share many characteristics with the fireballs in GRBs (Nakar, Piran, & Sari 2005), it was soon realized that those events can only accommodate a small fraction of the short hard burst population, perhaps 10% (Ofek 2006).

REFERENCES

Akerlof, C., et al. 1999, Nature, 398, 400
Akerlof, C., et al. 2000, ApJL, 532, L25
Band, D., et al. 1993, ApJ, 413, 281
Baring, M. G., & Harding, A. K. 1997, ApJ, 491, 663
Belczynski, K., et al. 2006, astro-ph/0601458
Beloboradov, A. 2000, ApJ, 539, 25
Berger, E., et al. 2000, ApJ, 545, 56
Berger, E., et al. 2003, Nature, 426, 154
Berger, E., et al. 2005, Nature, 438, 988
Bhat, P. N., et al. 1992, Nature, 359, 217
Blandford, R., & McKee, C. F. 1976, Phys. Fluids, 19, 1130
Bloom, J. S., et al. 1999, Nature, 401, 453
Bloom, J. S., et al. 2006, ApJ, 638, 354
Bremer, M., et al. 1998, A&A, 332, L13
Briggs, M. S., et al. 1999, ApJ, 524, 82
Burenin, R. A., et al. 2003, AsL, 29, 573
Castro-Tirado, A., et al. 1998, Science, 279, 1011
Castro-Tirado, A., et al. 1999, Science, 283, 2069
Chevalier, R. A., & Li, Z. 1999, ApJL, 520, L29
Chevalier, R. A., & Li, Z. 2000, ApJ, 536, 195
Costa, E., et al. 1997, Nature, 387, 783
Covino, S., et al. 2006, A&A, 447, L5
Eichler, D., et al. 1989, Nature, 340, 126
Fenimore, E. E., Epstein, R. I., & Ho, C. 1993, A&AS, 97, 59
Fenimore, E. E., Madras, C. D., & Nayakchin, S. 1996, ApJ, 473, 998
Fishman, G. J., & Meegan, C. A. 1995, ARA&A, 33, 415
Fox, D. B., et al. 2005, Nature, 437, 845

Frail, D. A., Waxman, E., & Kulkarni, S. R. 2000, ApJ, 537, 191
Frail, D. A., et al. 1997, Nature, 389, 261
Frail, D. A., et al. 2001, ApJ, 562, L55
Frail, D. A., et al. 2003, ApJ, 590, 992
Frail, D. A., et al. 2005, ApJ, 619, 994
Fruchter, A. S., et al. 1999, ApJL, 519, L13
Fruchter, A., et al. 2000, ApJ, 545, 664
Galama, T. J., et al. 1997, Nature, 387, 479
Galama, T. J., et al. 1998a, ApJL, 497, L13
Galama, T. J., et al. 1998b, ApJL, 500, L97
Galama, T. J., et al. 1998c, Nature, 395, 670
Galama, T. J., et al. 1999, Nature, 398, 394
Galama, T. J., et al. 2000, ApJ, 536, 185
Gal-Yam, A., et al. 2004, ApJ, 609, L59
Gherels, N., et al. 2005, Nature, 437, 851
Ghisellini, G., & Lazzati, D. 1999, MNRAS, 309, L7
Goodman, J. 1986, ApJL, 308, 46
Granot, J., Piran, T., & Sari, R. 1999, ApJL, 527, 236
Granot, J., Piran, T., & Sari, R. 2000a, ApJ, 513, 679
Granot, J., Piran, T., & Sari, R. 2000b, ApJ, 534, L163
Granot, J., & Sari, R. 2002, ApJ, 568, 820
Granot, et al. 2001, Proc. of the rome workshop 'Gamma-Ray Bursts in the Afterglow Era', ed. E. Costa, F. Frontera, & J. Hjorth, (Heidelberg: Springer-Verlag), 312
Granot, et al. 2005, ApJ, 618, 413
Greiner, J., et al. 2003, Nature, 426, 157
Gruzinov, A. 1999, ApJ, 525, L29
Gruzinov, A., & Waxman, E. 1999, ApJ, 511, 852
Harrison, F. A., et al. 1999, ApJL, 523, L121
Harrison, F. A., et al. 2001, ApJ, 559, 123
Hjorth, J., et al. 2005a, ApJ, 630, L117
Hjorth, J., et al. 2005b, Nature, 437, 859
Ioka, K., & Nakamura, T. 2001, ApJL, 554, 163
Iwamoto, K., et al. 1998, Nature, 395, 672
Jager, R., et al. 1993, Adv. Space Res., 13, 12, 315
Katz, J. I. 1994, ApJ, 422, 248
Kawabata, K., et al. 2003, ApJL, 593, 19
Kehoe, R., et al. 2001, ApJL, 554, L159
Kobayashi, S. 2000, ApJ, 545, 807
Kobayashi, S., Piran, T., & Sari, R. 1997, ApJ, 490, 92
Kobayashi, S., & Sari, R. 2001, ApJ, 551, 934
Kobayashi, S., et al. 2005, astro-ph/0506157
Kouveliotou, C., et al. 1993, ApJL, 413, L101
Krolik, J. H., & Pier, E. A. 1991, ApJ, 373, 277
Kulkarni, S. R., et al. 1998a, Nature, 393, 35
Kulkarni, S. R., et al. 1998b, Nature, 395, 663
Kulkarni, S. R., et al. 1999a, ApJ, 522, L97
Kulkarni, S. R., et al. 1999b, Nature, 398, 389
Kumar, P., & Piran, T. 2000a, ApJ, 532, 286
Kumar, P., & Piran, T. 2000b, ApJ, 535, 152
Lattimer, J. M., & Schramm, D. N. 1974, ApJL, 192, L145
Liang, E. P., et al. 1999, ApJL, 519, L21
Lipkin, Y. M., et al. 2004, ApJL, 606, 381
Lithwick, Y., & Sari, R. 2001, ApJ, 555, 540
Mészáros, P., & Rees, M. J. 1993, ApJ, 405, 278
Mészáros, P., & Rees, M. J. 1997, ApJ, 476, 232
Mészáros, P., & Rees, M. J. 1999a, MNRAS, 299, L10

Mészáros, P., & Rees, M. J. 1999b, MNRAS, 306, L39
Mészáros, P., Rees, M., & Wijers, R. A. M. J. 1998, ApJ, 499, 301
MacFadyen, A. I., Woosley, S. E. 1999, ApJ, 524, 262
Malesani, D., et al. 2004, ApJ, 609, L5
Mao, S., & Paczyński, B. 1992, ApJL, 388, L45
Mao, S., & Yi, I. 1994, ApJ, 424, L131
Matheson, T., et al. 2003, ApJ, 599, 394
Mazzali, P. A., et al. 2003, ApJL, 599 95
Medvedev, M. V., & Loeb, A. 1999, ApJ, 526, 697
Metzger, M. R., et al. 1997, Nature, 387, 879
Mirabel, N., et al. 2006, ApJ, 643, L99
Mochkovitch, R., et al. 1993, Nature, 361, 236
Moderski, R., Sikora, M., & Bulik, T. 2000, ApJ, 529, 151
Modjaz, M., et al. 2006, ApJ, 645, L21
Nakar, E., Gal-Yam, A., & Fox, D. B. 2006, astro-ph/0511254
Nakar, E., Granot, Y., & Gueta, D. 2004, ApJ, 606, 37
Nakar, E., & Piran, T. 2004, MNRAS, 53, 647
Nakar, E., & Piran, T. 2005, ApJL, 619 147
Nakar, E., Piran, P., & Sari, R. 2005, ApJ, 635, 516
Nakar, E., et al. 2006, ApJ, 640, 849
Narayan, R., & Paczyński, B. & Piran, T. 1992, ApJL, 395, L83
Narayan, R., et al. 2001, ApJ, 557, 949
Ofek, E. 2006, in preparation
Paczyński, B. 1986, ApJ, 308, L43
Paczyński, B. 1992, Nature, 355, 521
Paczyński, B. 1993, Ann. NY Acad. Sci. 688, 321
Paczyński, B. 1998, ApJL, 494, L45
Paczyński, B., & Rhoads, J. 1993, ApJ, 418, L5
Panaitescu, A. 2001, ApJ, 556, 1002
Panaitescu, A., & Kumar, P. 2001, ApJ, 554, 667
Panaitescu, A., & Kumar, P. 2002, ApJ, 571, 779
Panaitescu, A., & Kumar, P. 2004, MNRAS, 353, 511
Panaitescu, A., & Mészáros, P. 1998, ApJL, 493, L31
Panaitescu, A., & Mészáros, P. 1999, ApJ, 503, 314
Perna, R., Sari, R., & Frail, D. A. 2003, ApJ, 594, 379
Piran, T. 1999, Proc. of the Gräftåvallen workshop 'Gamma Ray Bursts: The First Three Minutes', ed. J. Poutanen & R. Svensson, (San Francisco: ASP), 3
Piro, L., Scarsi, L., & Butler, R. C. 1995, Proc. SPIE 2517, 169
Piro, L., et al. 1998, A&A, 331, L41
Postnov, K. A., Prokhorov, M. E., Lipunov, V. M. 2001, Astronomy Report, 45, 236
Quimby, R. M., et al. 2006, ApJ, 640, 402
Ramirez-Ruiz, E., & Fenimore, E. E. 1999, A&A, 138, 521
Rees, M. J., & Mészáros, P. 1994, ApJL, 403, L93
Reichart, D. E. 1997, ApJL, 485, L57
Reichart, D. E. 1999, ApJL, 521, 111
Rhoads, J. E. 1997, ApJL, 478, L1
Rhoads, J. E. 1999, ApJ, 525, 737
Rol, E., et al. 2000, ApJ, 544, 707
Rossi, E., Lazzati, D., & Rees, M. J. 2002, MNRAS, 332, 945
Rykoff, E., et al. 2004, ApJL, 601, L1013
Rykoff, E. S., et al. 2006, ApJL, 638, L5
Sahu, K. C., et al. 1997, Nature, 387, 476
Salmonson, J. 2001, ApJL, 546, L29
Sari, R. 1997, ApJL, 489, L37
Sari, R. 1998, ApJL, 494, L17
Sari, R. 1999, ApJ, 524, L43

Sari, R., Narayan, R., & Piran, T. 1996, ApJ, 473, 204
Sari, R., Piran, T., & Halpern, J. 1999, ApJ, 519, L17
Sari, R., Piran, T., & Narayan, R. 1998, ApJL, 497, L17
Sari, R., & Mészáros, P. 2000, ApJ, 535, L33
Sari, R., & Piran, T. 1995, ApJ, 455, L143
Sari, R., & Piran, T. 1997a, ApJ, 485, 270
Sari, R., & Piran, T. 1997b, MNRAS, 287, 110
Sari, R., & Piran, T. 1999a, ApJ, 520, 641
Sari, R., & Piran, T. 1999b, ApJL, 517, L109
Sari, R., & Piran, T. 1999c, A&A, 138, 537
Schaefer, B. E., & Walker, K. C. 1999, ApJL, 511, L89
Schmidt, M. 1999, ApJ, 523, L117
Schmidt, M. 2001, ApJ, 552, 36
Sheth, K., et al. 2003, ApJL, 595, 33
Smith, D. A., et al. 2003, ApJL, 596, 151
Soderberg, A. M., et al. 2004, Nature, 420, 649
Soderberg, A. M., et al. 2006, Nature, in press
Sollerman, J., et al. 2006, A&A, 454, 503
Stanek, K. Z., et al. 1999, ApJL, 522, L39
Stanek, K., et al. 2003, ApJL, 591, 17
Tan, J. C., Matzner, C. D., & McKee, C. F. 2001, ApJ, 551, 946
Taylor, et al. 2004, ApJL, 609, 1
Thomsen, B., et al. 2004, A&A, 419, L21
Tiengo, A., et al. 2003, A&A, 409, 983
Torii, K. et al. 2003, ApJL, 597, L101
Urata, Y. et al. 2004, ApJL, 601, 17
Van Paradijs, J., et al. 1997, Nature, 386, 686
Vietri, M. 1997, ApJ, 478, L9
Villasenor, J. S., et al. 2005, Nature, 437, 855
Watson, D., et al. 2004, ApJ, 605, 101
Waxman, E. 1997a, ApJL, 485, L5
Waxman, E. 1997b, ApJL, 491, L19
Wijers, R. A. M. J., & Galama, T. J. 1999, ApJ, 523, 177
Wijers, R. A. M. J., Rees, M. J., & Mészáros, P. 1997, MNRAS, 288, L51
Wijers, R. A. M. J., et al. 1999, ApJL, 523, L33
Woosley, S. E. 1993, ApJ, 405, 273
Woosley, S. E., Eastman, R. G., & Schmidt, B. P. 1999, ApJ, 516, 788
Yamazaki, R., Ioka, K., & Nakamura, T. 2004, ApJL, 607, 106
Yost, S. A., et al. 2002, ApJ, 577, 155
Yost, S. A., et al. 2003, ApJ, 597, 459
Zhang, B., & Mészáros, P. 2002, ApJ, 571, 876